Stem Cell Reports
Article

OPEN ACCESS

Human Clinical-Grade Parthenogenetic ESC-Derived Dopaminergic Neurons Recover Locomotive Defects of Nonhuman Primate Models of Parkinson's Disease

Yu-Kai Wang,[1,2,3,5] Wan-Wan Zhu,[1,5] Meng-Hua Wu,[1,4,5] Yi-Hui Wu,[1,2] Zheng-Xin Liu,[1] Ling-Min Liang,[1,3,4] Chao Sheng,[1] Jie Hao,[1,2,3] Liu Wang,[1,2,3,4] Wei Li,[1,2,3,4] Qi Zhou,[1,2,3,4,*] and Bao-Yang Hu[1,2,3,4,*]

[1]State Key Laboratory of Stem Cell and Reproductive Biology, Institute of Zoology, Chinese Academy of Sciences, Beijing 100101, China
[2]Institute for Stem Cell and Regeneration, Chinese Academy of Sciences, Beijing 100101, China
[3]Beijing Stem Cell Bank, Chinese Academy of Sciences, Beijing 100190, China
[4]University of Chinese Academy of Sciences, Beijing 100049, China
[5]Co-first author
*Correspondence: qzhou@ioz.ac.cn (Q.Z.), byhu@ioz.ac.cn (B.-Y.H.)
https://doi.org/10.1016/j.stemcr.2018.05.010

SUMMARY

Clinical application of stem cell derivatives requires clinical-grade cells and sufficient preclinical proof of safety and efficacy, preferably in primates. We previously successfully established a clinical-grade human parthenogenetic embryonic stem cell (hPESC) line, but the suitability of its subtype-specific progenies for therapy is not clear. Here, we compared the function of clinical-grade hPESC-derived midbrain dopaminergic (DA) neurons in two canonical protocols in a primate Parkinson's disease (PD) model. We found that the grafts did not form tumors and produced variable but apparent behavioral improvement for at least 24 months in most monkeys in both groups. In addition, a slight DA increase in the striatum correlates with significant functional improvement. These results demonstrated that clinical-grade hPESCs can serve as a reliable source of cells for PD treatment. Our proof-of-concept findings provide preclinical data for China's first ESC-based phase I/IIa clinical study of PD (ClinicalTrials.gov number NCT03119636).

INTRODUCTION

Neural progenies from human pluripotent stem cells (PSCs) premise the cure for neural degenerative diseases through cell replacement (Hu et al., 2010; Kriks et al., 2011; Ma et al., 2012a). In addition to human embryonic stem cells (ESCs) and induced pluripotent cells (iPSCs), human PSCs can also be generated from activated oocytes without sperm fertilization, which are called human parthenogenetic embryonic stem cells (hPESCs). Derivation of hPESCs does not destroy viable embryos, which makes these cells suitable for generating clinical-grade cell lines for therapy (Mai et al., 2007; Turovets et al., 2011). Despite the lack of paternal genomes, hPESCs are able to differentiate into neural stem cells and functional neuronal cells that maintain allele-specific expression of imprinted genes (Hao et al., 2009). These hPESC-derived neural stem cells engraft, survive, and promote behavioral recovery in rodent and primate models of neural degenerative diseases, such as Parkinson's disease (PD) (Sanchez-Pernaute et al., 2005). Because of the nature of parthenogenesis, hPESCs generate minimal immune complexity (major histocompatibility complex), and fewer hPESC lines can satisfy the required numbers of human leukocyte antigen (HLA) types for cell-based therapy of neurological diseases, such as PD (Espejel et al., 2014).

PD is the second most common progressive neurodegenerative disorder, and is primarily caused by the death of ventral mesencephalic dopaminergic (VM DA) neurons (Yoo et al., 2013). Transplantation of fetal VM DA neurons was beneficial in some PD patients (Freed et al., 2001; Lindvall et al., 1990; Olanow et al., 2003), which demonstrated the feasibility of cell transplantation-based therapy. Midbrain DA neurons of floor plate (FP) origin were successfully generated from hESCs and were functional in rodent and primate models of PD (Emborg et al., 2013b; Grealish et al., 2014; Hallett et al., 2015; Kriks et al., 2011; Ramos-Moreno et al., 2012), However, these cells produced variable behavioral improvements in PD monkeys (Emborg et al., 2013a; Sanchez-Pernaute et al., 2005). Likewise, DA neurons obtained from hPSCs using an embryoid body (EB) procedure also survived after transplantation in primate PD models (Emborg et al., 2013b). However, a direct comparison of the functional outcomes of DA neurons from these two protocols remains unavailable, especially in PD monkeys. Whether hPESCs can differentiate into subtype specialized DA neurons under current good manufacturing practice (CGMP) conditions, and whether such neuronal subtypes of parthenogenetic origin are able to correct the locomotive deficits in nonhuman primate models of PD, remain unknown.

We recently reported the derivation of clinical-grade hPESCs under CGMP conditions (Gu et al., 2017). The

present study employed this hPESC line (Q-CTS-hESC-1) and investigated its abilities for neural and neuronal differentiation, especially their potential to generate DA neurons. We also evaluated the safety and efficacy of these DA neurons in 1-methyl-4-phenyl-1,2,3,6-tetrahydropyridine (MPTP)-induced PD monkeys to identify optimal procedures for cell-based therapy of PD.

RESULTS

Clinical-Grade hPESCs Differentiate into Neural Epithelial Cells and Regional Specialized Neural Stem Cells

To examine whether the clinical-grade hPESCs Q-CTS-hESC-1 differentiate into neural lineage and DA neurons, we used well-established EB procedures for neural and neuronal differentiation of hESCs. Q-CTS-hESC-1 cells differentiate into early neuroepithelial cells (NE) on day 10 and organize into typical neural rosettes on days 15–18, similar to hESCs (Figure 1A). These NE cells exhibit a progressive transition from PAX6 expression on day 10 to PAX6 and SOX1 expression on day 15, which indicates conversion from primitive to definitive NE cells.

We also examined the expression of a rostral marker in these neural stem cells to determine whether Q-CTS-hESC-1 cells differentiated into regional specialized neural cells. On day 15, we detected the expression of OTX2 at high proportion in both groups of neural differentiation (Figures 1A and 1B), which indicates that the Q-CTS-hESC-1 cell-derived early NE cells differentiated into forebrain and midbrain cells.

Clinical-Grade hPESCs Differentiate into DA Neurons

To reveal whether the clinical-grade hPESCs could differentiate into neuronal subtypes such as DA neurons, we continued differentiating the Q-CTS-hESC-1 cell-derived NE cells via supplementation with additional morphogens, such as fibroblast growth factor 8 (FGF8). On day 42 of differentiation, the differentiated cells extended processes with elaborating branches, indicating the maturation of neurons. The differentiated neurons are positively labeled with markers of neuronal and midbrain DA neurons, such as TUJ1, FOXA2, and tyrosine hydroxylase (TH) (Figures 1A and 1B). qPCR analyses also demonstrated that these neurons express neural markers and midbrain DA-specific markers, such as *PAX6* on day 15 of neural differentiation, and *PITX3*, *NURR1*, and *TH* on day 42 of neuronal differentiation (Figure S1).

We also used the FP-based protocol to differentiate midbrain DA neurons directly from Q-CTS-hESC-1 cells. The rostral marker OTX2 was robustly induced on day 10. After 15 days of differentiation, we observed enrichment of the FP marker FOXA2 and the midbrain marker LMX1A, but not the dorsal forebrain precursor marker PAX6. By the end of the sixth week of differentiation, the Q-CTS-hESC-1 cells are differentiated into midbrain DA neurons and express markers of DA neurons (Figures 1C and 1D). To qualify these cells for clinical use, we conducted strict quality measures to test identity, sterility, activity, purity, and safety (Figure S2). Furthermore, these DA cells passed the certification of National Institutes for Food and Drug Control (NIFDC) of China (Table S1). These data suggest that we successfully generated GMP-compliant xeno-free clinical-grade derivatives. We investigated the ability of these differentiated DA neurons to fire action potentials using whole-cell clamping. At day 70 of differentiation, these DA neurons evoked whole-cell currents and could be blocked by tetrodotoxin (TTX) (Figures 1E and 1F). Repetitive action potentials were also observed in response to current injections (Figure 1G). Spontaneous action potentials were characterized by a high-frequency discharge and sharp spikes, and spontaneous postsynaptic currents that can also be abolished by TTX (Figure 1H). The percentage of neurons that exhibited a mature electrophysiology was 66.7% (n = 12). These results demonstrated that the clinical-grade hPESCs differentiated into mature DA neurons.

Clinical-Grade hPESC-Derived DA Neurons Survive and Migrate in Monkey Brains

To verify whether the clinical-grade hPESC-derived DA neurons could be used as a source of cells for PD therapy, we created monkey models of PD via unilateral intracarotid artery infusion of MPTP. After 11 months of behavioral evaluation, all 10 monkeys were used for transplantation. Committed DA neurons that were differentiated using the EB-based protocol or the FP-based protocol were transplanted into the right striatum of the MPTP-induced PD monkeys using stereotactic surgery (Table S2). To track the graft cells in monkey brains, we labeled the cells prior to transplantation with superparamagnetic iron oxide (SPIO) nanoparticles carrying rhodamine B, which is detectable using magnetic resonance imaging (MRI) or fluorescence microscopy. A total of 2 million cells were injected into both ends of the putamen and caudate of the striatum. Transplantation was verified using MRI scanning promptly after surgery, and the presence of detectable cell masses at the appropriate positions was deemed successful transplantation. At the ninth month after transplantation, the size of grafted cell mass in PD monkeys that received EB-DA or FP-DA neuron transplantation was not increased over time, as shown on MR images (Figure 2A). However, the volume of grafts is reduced to approximately half of the original volume according to MRI 9 months after transplantation (Figure 2B).

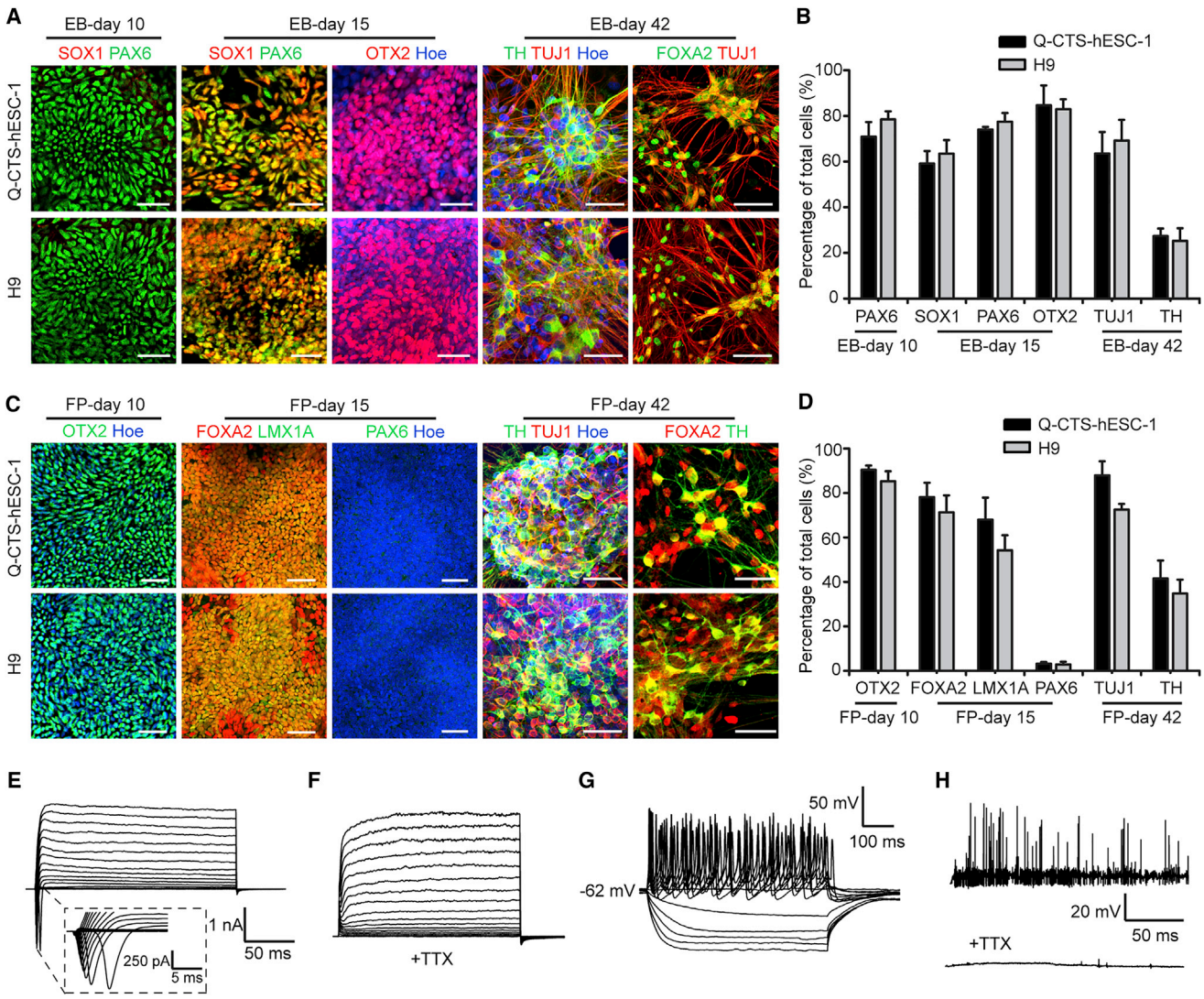

Figure 1. *In Vitro* Neural Induction of Clinical-Grade hPESC Q-CTS-hESC-1

(A) Immunofluorescence images of neural markers on days 10, 15, and 42 using EB protocol. n = 3 independent experiments. Scale bars, 50 μm.

(B) Quantification of the markers presented in (A). H9 was used as a control. Error bars indicate SEM; n = 3 independent experiments.

(C) Immunofluorescence images of neural markers on days 10, 15, and 42 using the FP protocol. n = 3 independent experiments. Scale bars, 50 μm.

(D) Quantification of the markers presented in (C). In (B) and (D), data are presented as mean ± SEM (compared with H9, Student's t test); n = 3 independent experiments.

(E–H) Electrophysiological analyses of DA neurons on day 70; n = 12 independent experiments.

(E) A representative example of Na^+ and K^+ currents recorded from hPESC-derived neurons.

(F) Na^+ currents were blocked by 1 μM tetrodotoxin (TTX).

(G) Representative action potentials recorded from hPESC-derived neurons in current-clamp mode.

(H) A representative trace of spontaneous action potentials sensitive to TTX treatment.

See also Figures S1 and S2; Table S1.

By the end of 9 months post transplantation, one or two monkeys from each group were euthanized for biopsy (Table S2). No cells were found at the site of transplantation in the control PD monkeys that did not receive cell transplantation. SPIO and rhodamine-labeled grafts were observed in the striatum in brain slices of monkeys that received cell transplantation (Figures 2C and 2D). A compact cell mass was surrounded by

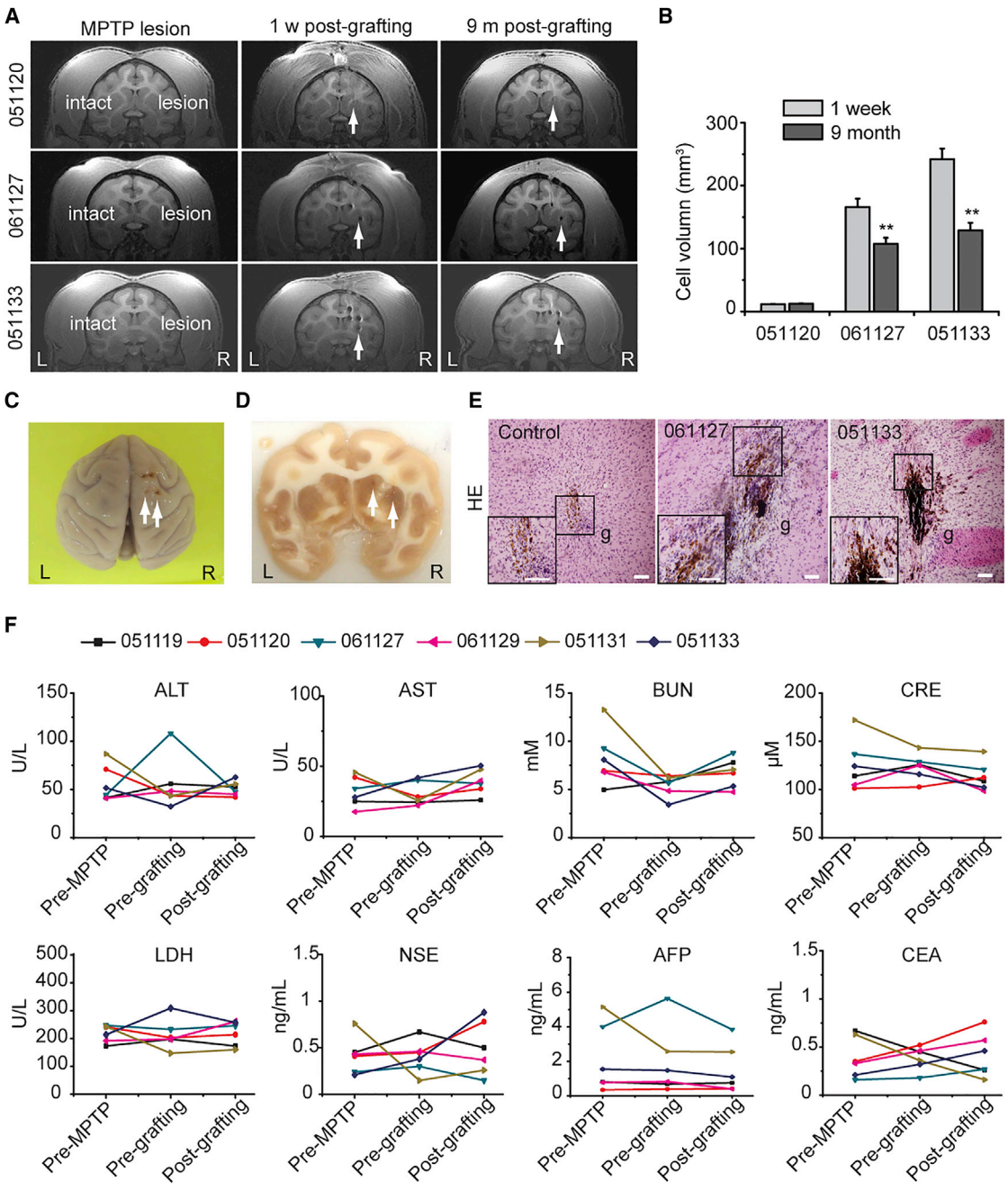

Figure 2. The Long-Term Surviving Transplants of hPESC-Derived DA Neurons Exhibited No Tumorigenicity

(A) Magnetic resonance imaging (MRI) scans of monkeys #051120 (control group), #061127 (EB-DA group), and #051133 (FP-DA group) implanted with day-42 FP-DA after MPTP lesion (left), 1 week post grafting (middle), and 9 months post grafting (right). The arrows indicate the grafts.

(B) Changes in the graft volumes of monkeys (#051120, #061127, and #051133) after cell transplantation for 1 week and 9 months estimated by MRI. Data are presented as mean ± SEM, n = 3. **p < 0.01 (Student's t test).

(C) Monkey brain tissues were obtained for biopsy analysis 9 months post transplantation. The arrows indicate the injection sites.

(D) Gross appearance of brain slice. SPIO-labeled grafts can be observed in striatum. The arrows indicate the injection sites.

(E) Histological analyses of brain slices with H&E staining. Scale bars, 500 μm.

(legend continued on next page)

sporadically localized migrating neurons at the injection site (Figure 2E).

Clinical-Grade hPESC-Derived Neurons Do Not Form or Cause Tumors

We observed no cell overgrowth in PD monkeys that received cell transplantation, but a detectable decrease in the grafted cell mass was observed using MRI. The reduced cell masses are partially due to cell migration from the transplantation sites, but this distribution was sparse and barely detectable using MRI (Figure 2B). In all six monkeys that were euthanized, brain organization remained normal at 9 months after cell transplantation and no tumors were found at the sites of cell transplantation (Figure 2E). Other areas outside the transplantation sites were also carefully examined in brain slices, and no positive findings were found. These results indicate that the grafted DA neurons did not form or induce tumors in brains.

To investigate whether the transplantation of clinical-grade hPESC-derived cells induce tumors in other places of the body, we scheduled all monkeys to receive physical examination and blood biochemistry for general biomarkers of tumors. During the 9-month follow-up, we did not find signs of tumor formation in any monkeys. Blood biochemistries revealed no significant alterations in α-fetoprotein, carcinoembryonic antigen, or other components after cell transplantation (Figure 2F and Table S3). No tumors were found in other organs of the PD monkeys that were euthanized and biopsied.

To analyze to what extent the immune response is induced in such a xenotransplantation setting, we examined HLA-D related (HLA-DR) and Iba1 using immunohistochemistry. Some microglia were identified surrounding the grafts, exhibiting ramified morphology (Figures S3A and S3B), which indicates moderate but tolerable immune response in the host brain (Ghosh, 2010; Kettenmann, 2006). These data indicated that the clinical-grade hPESC-derived neurons were relatively safe for potential therapeutic application.

Clinical-Grade hPESC-Derived Neural Cells Differentiate in Brains of PD Monkeys

To investigate whether the grafted DA neurons could further differentiate into mature and functional neurons in brains of the PD monkeys, we labeled the brain slices of the euthanized PD monkeys using Perl's Prussian blue staining or antibodies against markers of neuronal cells or DA neurons. In brain slices of PD monkeys that received cell transplantation, we found that cells with typical neuron morphology at the site of cell transplantation were stained by Perl's Prussian blue (Figure 3A). Histological analysis with diaminobenzidine (DAB) staining for TH showed very few TH^+ neurons and fibers at the sites of injection in PD monkeys that did not receive cells. However, robust TH^+ staining surrounding the sites of transplantation and substantial TH^+ fibers extending out from the grafts were observed in PD monkeys that received EB-DA or FP-DA neurons (Figure 3B). Immunofluorescence staining showed co-localization of rhodamine and the DA neuron marker TH (Figure 3C). The rhodamine-positive cells were also positive for human-specific neural cell adhesion molecule (hNCAM), which indicates that a large number (varying between 382,800 ± 262,221 and 947,290 ± 106,632 cells per animal, mean ± SEM, n = 3) of transplanted cells survived in the brain (Figures 3D and 3E). The proportion of TH^+ cells among survival cells varied between 5.2% and 8.1% (Figure 3E). In addition, Girk2-positive DA neurons were also detected in the grafts, indicating the presence of A9 DA neurons (Figures 3F and 3G).

Clinical-Grade hPESC-Derived Neurons Improve the Behavioral Performance of PD Monkeys

Next, we analyzed the effects of cell transplantation by rating the locomotor behavior of the PD monkeys. Precise body movements of the left side of each monkey were rated monthly in a double-blinded manner by experienced examiners, as described previously (Brownell et al., 1998; Ovadia et al., 1995). We compared differences between the control group (culture medium, n = 3), the EB-DA group (DA neurons differentiated through the EB-based protocol, n = 4), and the FP-DA group (midbrain DA neurons differentiated through the FP-based protocol, n = 3). Transplantation of FP- or EB-DA significantly alleviated PD symptoms (Figures 4A and S4A–S4C). The locomotive performance rating scores improved 59.5% and 53.8% at 8 months post transplantation in the two groups of monkeys that received EB-DA and FP-DA neurons, respectively (Figure 4B).

We also examined the behavioral alterations of each monkey in consideration of the significant individual variability. In each group, some monkeys reacted poorly to the transplantation, such as #051131 in the EB-DA group (Figure S4B). Improvement remained significant

(F) Blood examination results of all the monkeys pre-MPTP lesion, pre-grafting, and 9 months after grafting. ALT, alanine aminotransferase; AST, aspartate aminotransferase; BUN, blood urea nitrogen; CRE, creatinine; LDH, lactate dehydrogenase; NSE, neuron-specific enolase; AFP, α-fetoprotein; CEA, carcinoembryonic antigen.
See also Tables S2 and S3.

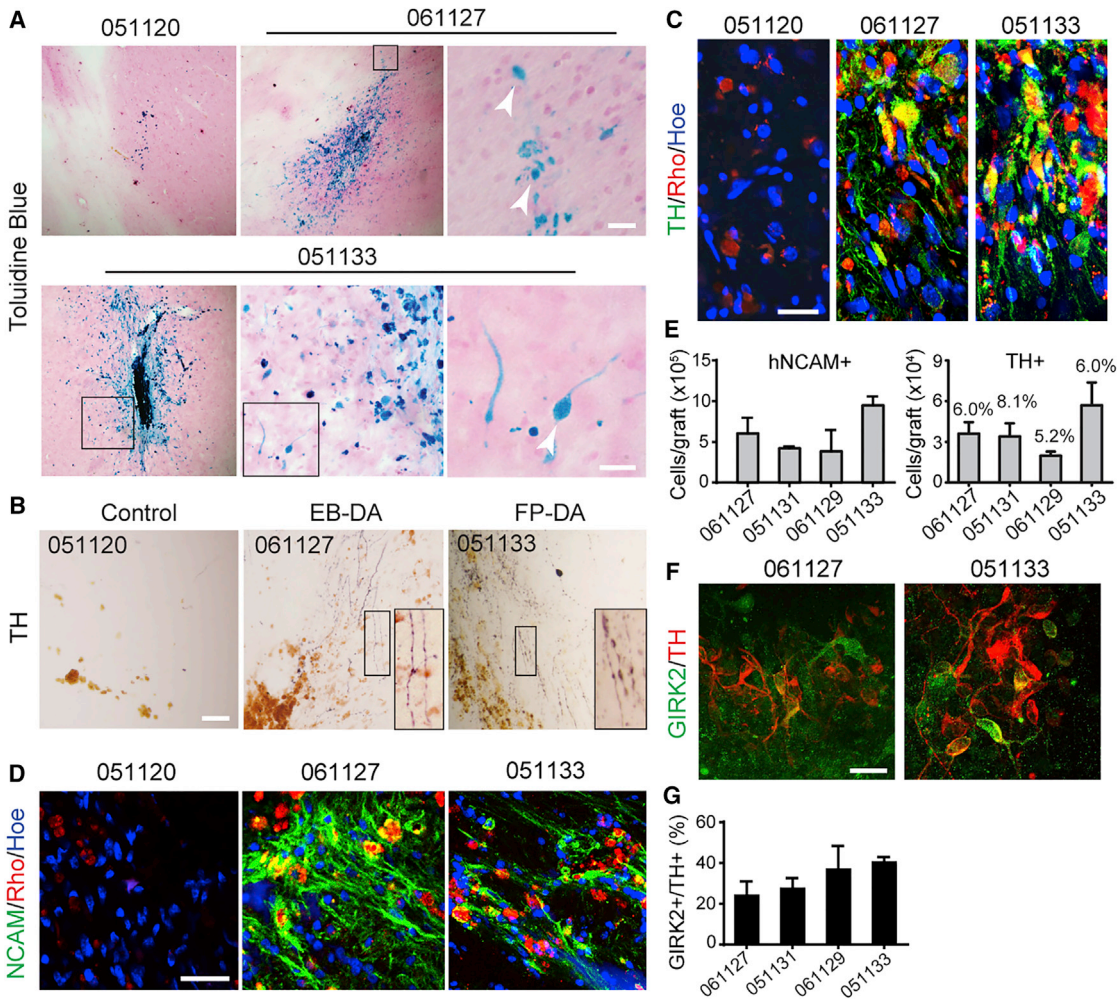

Figure 3. Phenotypes of Grafted hPESC-Derived DA Neurons 9 Months Post Grafting in MPTP-Induced PD Monkey Hosts

(A) Grafted neurons were labeled by Perl's Prussian blue staining. Robust survival and migration of dopamine neurons in the host brains were observed. The boxed area in each image is shown at a higher magnification on the right. Arrowheads indicate grafted neurons. Scale bar, 20 μm.

(B) Histological analysis using DAB-developed immunohistochemistry for tyrosine hydroxylase (TH) revealed numbers of TH^+ neurons dispersed throughout the graft, which is indistinguishable between the EB-DA and FP-DA groups. Scale bar, 200 μm.

(C and D) Expression of TH (C, green; scale bar, 20 μm) and human-specific neural marker NCAM (D, green; scale bar, 50 μm) co-localized with rhodamine (Rho, red).

(E) The number of $hNCAM^+$ cells and TH^+ cells surviving in each monkey. Data are presented as mean ± SEM, n = 3.

(F) Immunostaining for TH (red) and co-expression (green) with GIRK2. Scale bar, 20 μm.

(G) The percentage of $GIRK2^+$ cells per TH^+ DA neuron. Data are presented as mean ± SEM, n = 3.

See also Figure S3.

and stable over time for some monkeys, such as #041125 in the EB-DA group and #051123 in the FP-DA group, which exhibited 66.7% and 42.3% improvement, respectively at the end of 8 months. Notably, this behavioral improvement was sustained for at least 24 months, which supports the long-term function of these grafted cells in the brain (Figures S4B and S4C). The maximum behavioral improvement occurred in #061127 of the EB-DA group, in which a 69.2% improvement occurred within 2 months after transplantation. The effect diminished during the subsequent 6 months, and the improvement was 23.1% at the end of 8 months (Figure S4B). In either the EB-DA group or the FP-DA group, the most significant behavioral improvement occurred between the first and fourth months after transplantation (Figures S4B and S4C).

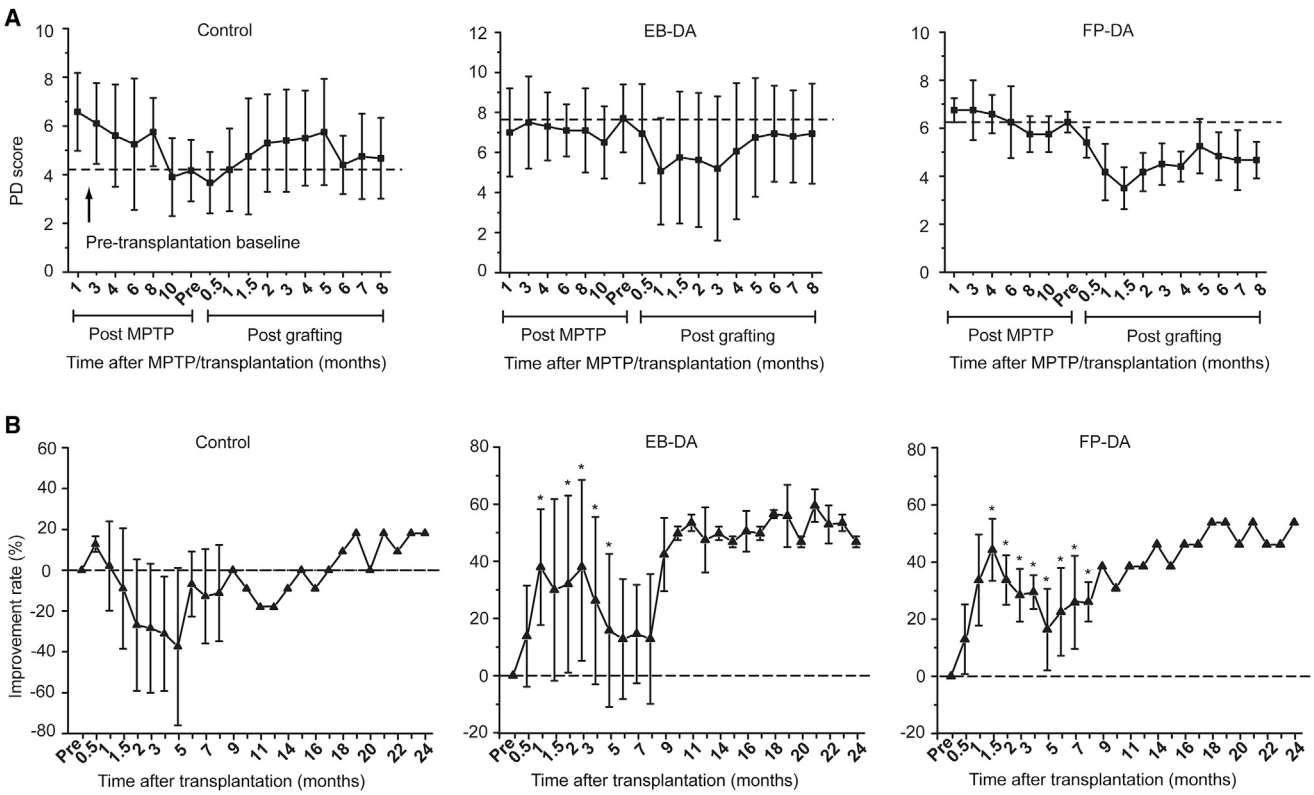

Figure 4. Behavioral Evaluation in Monkeys after Transplantation of EB-DA and FP-DA Neurons

(A) Time course of changes in motor symptom scores of the monkeys injected with culture medium (control group, n = 3), EB-DA neurons (EB-DA group, n = 4), and FP-DA neurons (FP-DA group, n = 3) from MPTP administration to 8 months after transplantation.

(B) Behavioral improvement rate of the three groups after transplantation (0–24 months), which revealed a significant increase in the two groups that received EB-DA or FP-DA neurons. Dotted lines are pre-transplantation baseline scores 11 months after MPTP treatment. Significance compared with control group (Student's t test): *$p < 0.05$.

Data are represented as means ± SEM (n = 3 animals for the control and FP-DA groups, 4 animals for the EB-DA group). See also Figure S4.

Monkeys #051118 and #051119 in the control group exhibited temporary behavioral improvement in the first 2 months post transplantation, which indicates spontaneous behavioral recovery following the surgery itself (Figure S4A). Therefore, the behavioral improvement during the first 2 months may reflect the overall effects of spontaneous recovery, regardless of whether monkeys received cell transplantation or not.

Dopamine Level in the Putamen or CN Is Critical for Behavioral Improvement

To further investigate the mechanism of behavioral improvement of cell therapy, we focused on two monkeys that exhibited the greatest benefit from the cell transplantation, #051131 and #051133. We collected tissue samples of striatum that contained grafted DA neurons. Levels of dopamine and 5-hydroxytryptamine (5-HT, control) were measured using high-performance liquid chromatography (HPLC) (Figure S5A). In all groups, dopamine was readily detected in the putamen and caudate nucleus (CN) in brain tissues from the control side (Figures 5A–5D, S5B, and S5C). Dopamine was not detected in samples from the lesion side of the brain in monkey #051120 (control group) or #051131 (EB-DA group) (Figures 5A, 5B, S5B, and S5C). However, an obvious increase in dopamine was observed in the posterior site of the CN (Figure 5C) and the anterior site of the putamen in the monkey that received FP-DA transplantation (#051133) (Figure 5D). Notably, monkey #051133 exhibited significant behavioral improvement before the date of euthanasia.

Precise Targeting in the Putamen or CN Affected DA Levels and Behavior

To find out why DA neuron transplantation generated variable outcomes, we carefully investigated the correlation of MRI, dopamine level, and behavioral improvement. Monkeys that exhibited significant behavioral improvement and elevated dopamine levels contained grafted DA

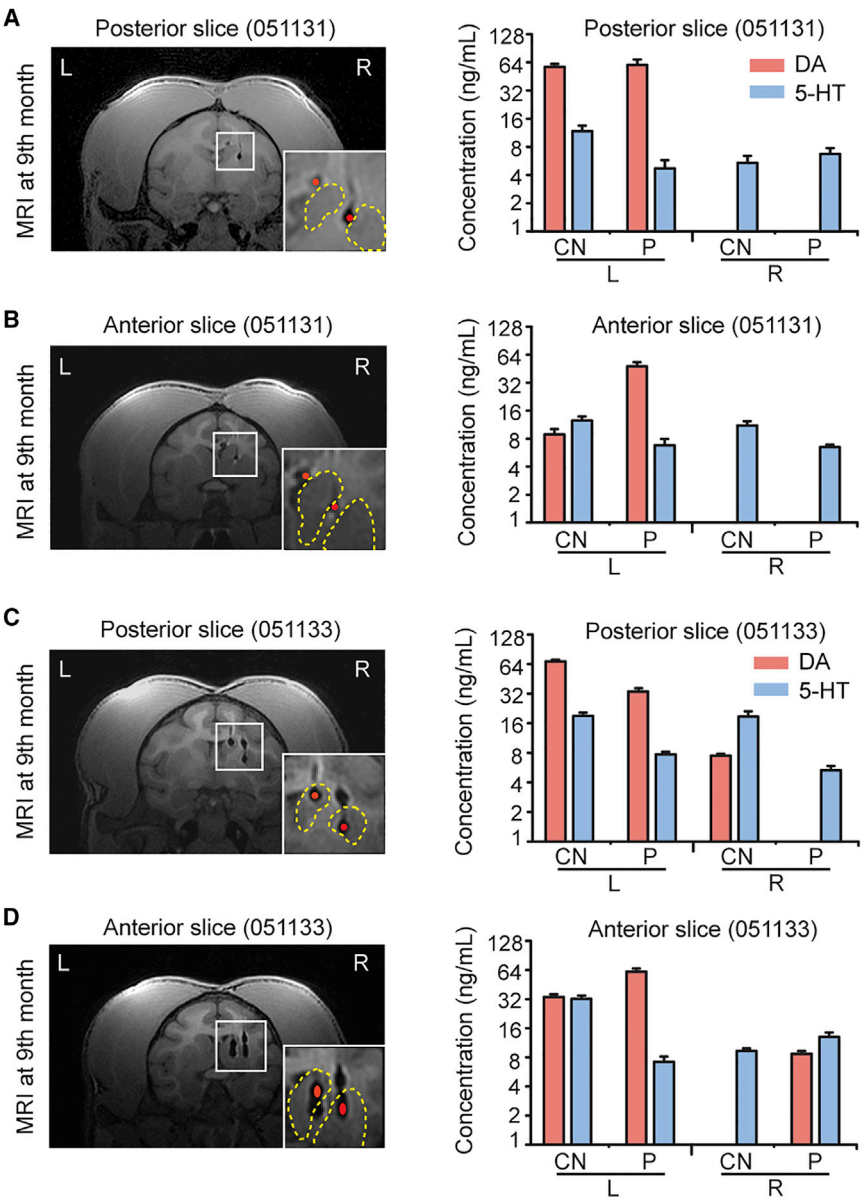

Figure 5. *In Vivo* Functional Characterization of Grafted Neurons in Putamen and Caudate Nucleus Measured by HPLC

Left panels: MRI images of the monkey brains (051131, A and B, and 051133, C and D) at 9 months. The red dots represent the graft. The yellow dashed lines delineate the putamen and caudate nucleus. Right panels: Levels of DA in the putamen (P) and caudate nucleus (CN). 5-Hydroxytryptamine (5-HT) was measured as a control (n = 3 repeated experiments). The rostral and caudal injection sites are shown in the anterior and posterior slices, respectively.

Data are represented as means ± SEM (n = 3 repeated experiments). See also Figure S5.

neurons precisely located at the putamen or CN (Figures 5C and 5D). Therefore, the precise targeting into the striatum was important to the overall outcomes of transplantation.

DISCUSSION

In this study, we differentiated clinical-grade hPESCs into subtype-specific DA neurons under CGMP conditions and demonstrated their therapeutic potential in PD monkeys. The hPESC line we chose and the materials we used for differentiation were both accredited by the China Food and Drug Administration (CFDA). Notably, the biosafety and effectiveness of differentiated DA cells were validated by NIFDC, the subordinate institution for drug and food safety evaluations of CFDA. We demonstrated that neither the clinical-grade conditions of DA neuron generation nor the parthenogenetic nature of hPESCs significantly influenced DA differentiation or affected the efficacy of differentiated DA neurons in the treatment of PD monkeys. These results support the translation of these transplantations into clinical application.

Human ESCs can be differentiated into DA neurons using protocols of various strategies (Chambers et al., 2009; Morizane et al., 2010; Pankratz et al., 2007; Xi et al., 2012). The present study differentiated hPESCs using two protocols,

which we called "EB protocol" and "FP protocol" (Kriks et al., 2011; Ma et al., 2011). Double-blind analysis of the locomotive behavior demonstrated very little difference between these two groups, suggesting that DA neurons generated with these two protocols are functionally equivalent for transplantation (Liu et al., 2013; Ma et al., 2012b).

The lack of long-term studies on safety and efficacy in primates would hardly support the use of ESC-derived progenies in practice (Gonzalez et al., 2015; Morizane et al., 2013). Our results demonstrated that cells labeled with iron oxide nanoparticles were detectable in all brains that received transplantation, and TH^+ cells were well distributed around the site of injection, indicating the integration of graft cells into the recipient brain. No graft-derived overgrowths, or signs of other tumor formation were observed in monkeys that received cell transplantation during our 9-month follow-up of cell transplantation. Neither positive macrophages/activated microglia nor inactive microglia surrounded the grafts, which suggests little inflammation and damage in the brain (Emborg et al., 2013a; Roggendorf et al., 1996; Vogel et al., 2013). These data suggest that the clinical-grade hPESC-derived DA neurons can be potentially used for therapy.

We noted that improvements in locomotive behavior varied significantly between individual monkeys, and monkeys in which the DA neurons were accurately grafted into putamen and CN tended to exhibit better performance. This result is consistent with previous studies in rodents and primates (Doi et al., 2012; Grealish et al., 2014; Hallett et al., 2015; Kikuchi et al., 2017). Our data also demonstrated that the dopamine level in putamen or CN may be a sensitive indicator of the behavioral improvements of cell therapy. These findings are consistent with a previous report that DA concentrations in striatum highly correlate with behavior scores (Gonzalez et al., 2016).

Notably, we observed rapid recoveries in most monkeys immediately after the surgery, including monkeys that did not receive transplantation. This result suggests that the surgery itself also contributed to the behavioral recovery during the first 2 months. Therefore, timing should be taken into consideration to evaluate the efficacy of cell transplantation, and only alterations that occur 2 months post transplantation may reflect the therapeutic effect of graft cells. These results clearly support precise transplantation of hPESC-derived DA neurons into striatum as a promising approach for the treatment of PD patients.

EXPERIMENTAL PROCEDURES

hPESC Culture

hPESC line Q-CTS-hESC-1 established on human clinical-grade feeder cells under GMP standard (Fink, 2009; Hyun et al., 2008; Wilkerson et al., 2013) was used in conformity with "The Guidelines for Research and Ethic of Human Embryonic Stem Cells" of the Ministry of Science and Technology and National Health and Family Planning Commission of the People's Republic of China (NHFPC). Undifferentiated Q-CTS-hESC-1 cell (passages 25–40) was maintained in Essential 8 (E8) medium on vitronectin-coated dishes under clinical-grade standards, as reported previously (Gu et al., 2017).

Induction of DA Neurons from ESCs *In Vitro*

Dopaminergic neural cells were differentiated following one of the two protocols published previously. Q-CTS-hESC-1 and H9 cells in the EB-based method (Ma et al., 2011) were lifted with Dispase (1.5 U/mL, Gibco) for aggregates in hESC medium for 4 days and were shifted to a chemically defined neural induction medium (NIM) containing DMEM/F12, N2, nonessential amino acids and heparin (2 μg/mL, Sigma) for 2 days. The cell aggregates were attached to a growth surface for rosette formation and colony selection for another week. Columnar cells in the center of colonies were mechanically separated and grown as floating neural spheres in NIM for DA neuron differentiation in the presence of SHH C25II (100 ng/mL, R&D Systems) and FGF8 (50 ng/mL, Peprotech). On days 23–25 of differentiation, the neuroepithelial clusters were plated onto PO/laminin/fibronectin-coated dishes with neural differentiation medium supplemented with 1 mM cyclic AMP (cAMP; Sigma), 0.2 mM ascorbic acid (Sigma), 1 mg/mL laminin (Sigma), 1 ng/mL transforming growth factor β3 (TGFβ3; Peprotech), 10 ng/mL brain-derived neurotrophic factor (BDNF; Peprotech), and 10 ng/mL glial cell line-derived neurotrophic factor (GDNF; Peprotech). For the FP-based method (Kriks et al., 2011), Q-CTS-hESC-1 and H9 cells were dissociated into single cells with Tryple (Invitrogen) and plated onto Matrigel-coated dishes. The dissociated cells were cultured on Matrigel (BD Biosciences) in DMEM/F12 containing 2 mM L-Glutamax and 10 mM β-mercaptoethanol supplemented with 100 nM LDN193189 (Stemgent), 10 μM SB431542 (Stemgent), 100 ng/mL SHH C25II (R&D), 2 μM purmorphamine (Stemgent), 100 ng/mL FGF8 (Peprotech), and 3 μM CHIR99021 (Stemgent). On day 11, medium was changed to NDM supplemented with CHIR99021 (until day 13), and with BDNF, GDNF, TGFβ3, and dibutyryl cAMP for 9 days. On day 21, cells were dissociated using Tryple and replated with a high cell density on dishes pre-coated with PO/laminin/fibronectin in NDM with five factors, until they matured to DA neuron stage for transplantation.

Animals

Ten adult male cynomolgus monkeys (5.5–7.5 kg, 6–8 years old) were housed in single quarters with a 12:12-hr light/dark cycle. Animals were provided with monkey chow and enrichment food twice a day and water *ad libitum*. The monkey models were randomly divided into three groups (group 1: #041125, #061127, #061128, #051131 for day-42 EB-DA neuron grafts; group 2: #051123, #061129, #051133 for day-42 FP-DA neuron grafts; group 3: #051118, #051119, #051120 for culture medium).

The animal experiments were performed at Wincon TheraCells Biotechnologies (Guangxi, China), which is an AAALAC-accredited nonhuman primate research facility. The protocols were approved by the Institutional Animal Care and Use Committee

(IACUC). All efforts were made to minimize the number of animals used and to ameliorate any distress.

MPTP Administration

The animal was placed on a heated blanket, and cardiac and respiratory parameters were monitored during the procedure. The animal was placed in the supine position with the neck hyperextended and head slightly turned to the left. MPTP was administered to the right hemisphere of the monkeys. Once the common carotid artery (CCA) was exposed, the external carotid artery was temporally blocked by a micro-bulldog clamp to occlude blood flow. All of the CCA blood flow was diverted into the internal carotid artery. A 25-gauge butterfly needle, attached to a syringe with previously mixed MPTP solution (3 mg of MPTP-HCl in 20 mL of saline), was bent at the tip to a slight angle, than inserted retrograde to the blood flow through the CCA wall and into the CCA lumen. The MPTP solution was delivered at a rate of 1.33 mL/min. The animals remained stable with an increase in heart rate (up to 20–30 counts/min) during this time. The dose and volume of MPTP was confirmed at the end of the surgery. In addition, ipsilateral mydriasis and muscle tension of contralateral limbs were immediately examined and recorded in the surgery notes of all animals (Ding et al., 2008; Luan et al., 2008).

Behavioral Evaluation

Video recordings of all monkeys were analyzed using an automated video-tracking system. Motor symptoms were assessed from the videos using a rating scale for parkinsonian monkeys that was modified from the section III (motor examination) of the human Unified Parkinson's Disease Rating Scale (Brownell et al., 1998; Ovadia et al., 1995). In brief, the videos were evaluated blindly by a trained examiner in the following categories: tremor (0–3), bradykinesia (0–3), rigidity (0–3), posture (0–3), balance (0–3), and motor skills (0–3). Minimum score is 0, indicating a normal monkey, whereas maximum score 18 indicates an animal with severe PD symptoms. The rating scale data collected every month post MPTP surgery and post cell transplantation were used to show the stability of the PD features.

Cell Labeling

For tracking purposes, DA neural cells were labeled prior to cell transplantation with Molday ION rhodamine B (MIRB; Biopal). MIRB is a new SPIO-based MRI contrast reagent with a colloidal size of 35 nm. This colloid is specifically designed for cell labeling and MRI tracking and does not require transfection reagents for efficient cell labeling. This SPIO is crosslinked for stability and labeled with the fluorescent dye rhodamine B. MIRB can be visualized by both MRI (T2 imaging agents) and fluorescence. The solutions containing MIRB (25 μg/mL) were added to culture medium and incubated for 12 hr. Cells were then washed three times with PBS promptly before transplantation. After the third round of washing, the PBS was filtered to remove any remaining cells and was used as negative control of transplantation.

Cell Transplantation

Monkeys received MRI-guided stereotactic intracerebral injections of neurons 10–12 months after MPTP administration, according to previously published protocols (Emborg et al., 2008; Xi et al., 2012). The animals received two injections of a suspension containing 50,000 cells/μL in the caudate (volume: rostral 10 μL, caudal 10 μL) and two injections in the putamen (volume: rostral 10 μL, caudal 10 μL). The cells were delivered at a rate of 1 μL/min using a 20-gauge Hamilton needle. The needle remained in place for an additional 10 min after completion of the injection. Monkeys received daily administrations of cyclosporine A (8 mg/kg orally, bolus gavage) 2 days prior to cell implantation and every 2 days for 2 weeks post grafting. The monkeys were gently handled for drug administration using a pole and collar system as previously described (Emborg et al., 2008; Sanchez-Pernaute et al., 2005).

Magnetic Resonance Imaging Location

MRI was performed 1 week before and every month after cell transplantation. Cynomolgus monkeys were pre-medicated with atropine (0.025 mg/kg subcutaneously) and anesthetized using isoflurane. Animals were installed in a stereotaxic frame and placed in the Magnetom Vision 1.5 T MR scanner (Siemens, Germany). T2-weighted sequences, previously employed for the detection of MIRB-labeled cells (Kim et al., 2009), were applied to assess MRI sensitivity to MIRB-labeled DA neural cells. The segment images for the graft were used to calculate graft volumes.

Postmortem Morphology and Neurochemistry

Approximately 9 months after cell transplantation, 6 of the 10 animals were deeply anesthetized with pentobarbital and euthanized via transcranial perfusion of ice-cold saline followed by 4% paraformaldehyde (pH 7.4) for 24 hr. The brain was then resuspended in a graded 30% sucrose solution and sliced into 40-μm serial sections on a freezing microtome. The brain sections were used for immunohistochemical staining according to published protocols (Emborg et al., 2001).

HPLC

Multiple tissue punches were taken from both sides of the CN and putamen containing the graft sites. Levels of DA and 5-HT were measured in the punches by HPLC coupled with electrochemical detection as described previously (Studer et al., 1996).

Statistical Analyses

Statistical analyses were performed using GraphPad Prism (San Diego, CA) software. Results are presented as mean ± SEM. The differences were calculated by Student's t test to compare the EB-DA or FP-DA group against the control group. Differences of $p < 0.05$ were considered significant.

SUPPLEMENTAL INFORMATION

Supplemental Information includes Supplemental Experimental Procedures, five figures, and three tables and can be found with this article online at https://doi.org/10.1016/j.stemcr.2018.05.010.

AUTHOR CONTRIBUTIONS

Q.Z. and B.-Y.H. designed the research. Y.-K.W., W.-W.Z., M.-H.W., L.-M.L., Y.-H.W., C.S., and Z.-X.L. performed the research and

collected data. J.H., L.W., and W.L. contributed new reagents and analytic tools. Y.-K.W. and W.-W.Z. analyzed the data. Y.-K.W., W.-W.Z., and B.-Y.H. wrote the manuscript.

ACKNOWLEDGMENTS

We thank S.-W. Li, X.-L. Zhu, and Q. Meng for their technical support in confocal laser-scanning microscopy and fluorescence-activated cell sorting. This work was supported by grants from the Program of National Key Research and Development (2016YFA0101402 and 2017YFA0105002); the National Basic Research Program of China (2014CB964604 and 2012CBA01300); the Key Deployment Projects of the Chinese Academy of Sciences (ZDRW-ZS-2017-5); the National Natural Science Foundation of China (31621004 and 31571533); the Key Research Projects of the Frontier Science of the Chinese Academy of Sciences (QYZDY-SSW-SMC002); and the Beijing Science and Technology Major Project (Z181100001818002).

Received: January 10, 2018
Revised: May 18, 2018
Accepted: May 18, 2018
Published: June 14, 2018

REFERENCES

Brownell, A.L., Jenkins, B.G., Elmaleh, D.R., Deacon, T.W., Spealman, R.D., and Isacson, O. (1998). Combined PET/MRS brain studies show dynamic and long-term physiological changes in a primate model of Parkinson disease. Nat. Med. *4*, 1308–1312.

Chambers, S.M., Fasano, C.A., Papapetrou, E.P., Tomishima, M., Sadelain, M., and Studer, L. (2009). Highly efficient neural conversion of human ES and iPS cells by dual inhibition of SMAD signaling. Nat. Biotechnol. *27*, 275–280.

Ding, F., Luan, L., Ai, Y., Walton, A., Gerhardt, G.A., Gash, D.M., Grondin, R., and Zhang, Z. (2008). Development of a stable, early stage unilateral model of Parkinson's disease in middle-aged rhesus monkeys. Exp. Neurol. *212*, 431–439.

Doi, D., Morizane, A., Kikuchi, T., Onoe, H., Hayashi, T., Kawasaki, T., Motono, M., Sasai, Y., Saiki, H., Gomi, M., et al. (2012). Prolonged maturation culture favors a reduction in the tumorigenicity and the dopaminergic function of human ESC-derived neural cells in a primate model of Parkinson's disease. Stem Cells *30*, 935–945.

Emborg, M.E., Shin, P., Roitberg, B., Sramek, J.G., Chu, Y., Stebbins, G.T., Hamilton, J.S., Suzdak, P.D., Steiner, J.P., and Kordower, J.H. (2001). Systemic administration of the immunophilin ligand GPI 1046 in MPTP-treated monkeys. Exp. Neurol. *168*, 171–182.

Emborg, M.E., Ebert, A.D., Moirano, J., Peng, S., Suzuki, M., Capowski, E., Joers, V., Roitberg, B.Z., Aebischer, P., and Svendsen, C.N. (2008). GDNF-secreting human neural progenitor cells increase tyrosine hydroxylase and VMAT2 expression in MPTP-treated cynomolgus monkeys. Cell Transplant. *17*, 383–395.

Emborg, M.E., Liu, Y., Xi, J., Zhang, X., Yin, Y., Lu, J., Joers, V., Swanson, C., Holden, J.E., and Zhang, S.C. (2013a). Induced pluripotent stem cell-derived neural cells survive and mature in the nonhuman primate brain. Cell Rep. *3*, 646–650.

Emborg, M.E., Zhang, Z., Joers, V., Brunner, K., Bondarenko, V., Ohshima, S., and Zhang, S.C. (2013b). Intracerebral transplantation of differentiated human embryonic stem cells to hemiparkinsonian monkeys. Cell Transplant. *22*, 831–838.

Espejel, S., Eckardt, S., Harbell, J., Roll, G.R., McLaughlin, K.J., and Willenbring, H. (2014). Brief report: parthenogenetic embryonic stem cells are an effective cell source for therapeutic liver repopulation. Stem Cells *32*, 1983–1988.

Fink, D.W. (2009). FDA regulation of stem cell-based products. Science *324*, 1662–1663.

Freed, C.R., Breeze, R.E., and Fahn, S. (2001). Transplantation of embryonic dopamine neurons for severe Parkinson's disease. N. Engl. J. Med. *345*, 146, author reply 147.

Ghosh, A. (2010). Brain APCs including microglia are only differential and positional polymorphs. Ann. Neurosci. *17*, 191–199.

Gonzalez, R., Garitaonandia, I., Crain, A., Poustovoitov, M., Abramihina, T., Noskov, A., Jiang, C., Morey, R., Laurent, L.C., Elsworth, J.D., et al. (2015). Proof of concept studies exploring the safety and functional activity of human parthenogenetic-derived neural stem cells for the treatment of Parkinson's disease. Cell Transplant. *24*, 681–690.

Gonzalez, R., Garitaonandia, I., Poustovoitov, M., Abramihina, T., McEntire, C., Culp, B., Attwood, J., Noskov, A., Christiansen-Weber, T., Khater, M., et al. (2016). Neural stem cells derived from human parthenogenetic stem cells engraft and promote recovery in a nonhuman primate model of Parkinsons disease. Cell Transplant. *25*, 1945–1966.

Grealish, S., Diguet, E., Kirkeby, A., Mattsson, B., Heuer, A., Bramoulle, Y., Van Camp, N., Perrier, A.L., Hantraye, P., Bjorklund, A., et al. (2014). Human ESC-derived dopamine neurons show similar preclinical efficacy and potency to fetal neurons when grafted in a rat model of Parkinson's disease. Cell Stem Cell *15*, 653–665.

Gu, Q., Wang, J., Wang, L., Liu, Z.X., Zhu, W.W., Tan, Y.Q., Han, W.F., Wu, J., Feng, C.J., Fang, J.H., et al. (2017). Accreditation of biosafe clinical-grade human embryonic stem cells according to Chinese regulations. Stem Cell Rep. *9*, 366–380.

Hallett, P.J., Deleidi, M., Astradsson, A., Smith, G.A., Cooper, O., Osborn, T.M., Sundberg, M., Moore, M.A., Perez-Torres, E., Brownell, A.L., et al. (2015). Successful function of autologous iPSC-derived dopamine neurons following transplantation in a non-human primate model of Parkinson's disease. Cell Stem Cell *16*, 269–274.

Hao, J., Zhu, W., Sheng, C., Yu, Y., and Zhou, Q. (2009). Human parthenogenetic embryonic stem cells: one potential resource for cell therapy. Sci. China C Life Sci. *52*, 599–602.

Hu, B.Y., Weick, J.P., Yu, J., Ma, L.X., Zhang, X.Q., Thomson, J.A., and Zhang, S.C. (2010). Neural differentiation of human induced pluripotent stem cells follows developmental principles but with variable potency. Proc. Natl. Acad. Sci. USA *107*, 4335–4340.

Hyun, I., Lindvall, O., Ahrlund-Richter, L., Cattaneo, E., Cavazzana-Calvo, M., Cossu, G., De Luca, M., Fox, I.J., Gerstle, C., Goldstein, R.A., et al. (2008). New ISSCR Guidelines underscore major principles for responsible translational stem cell research. Cell Stem Cell *3*, 607–609.

Kettenmann, H. (2006). Triggering the brain's pathology sensor. Nat. Neurosci. *9*, 1463–1464.

Kikuchi, T., Morizane, A., Doi, D., Magotani, H., Onoe, H., Hayashi, T., Mizuma, H., Takara, S., Takahashi, R., Inoue, H., et al. (2017). Human iPS cell-derived dopaminergic neurons function in a primate Parkinson's disease model. Nature *548*, 592–596.

Kim, S.H., Lee, W.J., Lim, H.K., and Park, C.K. (2009). SPIO-enhanced MRI findings of well-differentiated hepatocellular carcinomas: correlation with MDCT findings. Korean J. Radiol. *10*, 112–120.

Kriks, S., Shim, J.W., Piao, J., Ganat, Y.M., Wakeman, D.R., Xie, Z., Carrillo-Reid, L., Auyeung, G., Antonacci, C., Buch, A., et al. (2011). Dopamine neurons derived from human ES cells efficiently engraft in animal models of Parkinson's disease. Nature *480*, 547–551.

Lindvall, O., Brundin, P., Widner, H., Rehncrona, S., Gustavii, B., Frackowiak, R., Leenders, K.L., Sawle, G., Rothwell, J.C., Marsden, C.D., et al. (1990). Grafts of fetal dopamine neurons survive and improve motor function in Parkinson's disease. Science *247*, 574–577.

Liu, Y., Weick, J.P., Liu, H.S., Krencik, R., Zhang, X.Q., Ma, L.X., Zhou, G.M., Ayala, M., and Zhang, S.C. (2013). Medial ganglionic eminence-like cells derived from human embryonic stem cells correct learning and memory deficits. Nat. Biotechnol. *31*, 440–447.

Luan, L., Ding, F., Ai, Y., Andersen, A., Hardy, P., Forman, E., Gerhardt, G.A., Gash, D.M., Grondin, R., and Zhang, Z. (2008). Pharmacological MRI (phMRI) monitoring of treatment in hemiparkinsonian rhesus monkeys. Cell Transplant. *17*, 417–425.

Ma, L., Hu, B., Liu, Y., Vermilyea, S.C., Liu, H., Gao, L., Sun, Y., Zhang, X., and Zhang, S.C. (2012a). Human embryonic stem cell-derived GABA neurons correct locomotion deficits in quinolinic acid-lesioned mice. Cell Stem Cell *10*, 455–464.

Ma, L., Liu, Y., and Zhang, S.C. (2011). Directed differentiation of dopamine neurons from human pluripotent stem cells. Methods Mol. Biol. *767*, 411–418.

Ma, L.X., Hu, B.Y., Liu, Y., Vermilyea, S.C., Liu, H.S., Gao, L., Sun, Y., Zhang, X.Q., and Zhang, S.C. (2012b). Human embryonic stem cell-derived GABA neurons correct locomotion deficits in quinolinic acid-lesioned mice. Cell Stem Cell *10*, 455–464.

Mai, Q.Y., Yu, Y., Li, T., Wang, L., Chen, M.J., Huang, S.Z., Zhou, C.Q., and Zhou, Q. (2007). Derivation of human embryonic stem cell lines from parthenogenetic blastocysts. Cell Res. *17*, 1008–1019.

Morizane, A., Darsalia, V., Guloglu, M.O., Hjalt, T., Carta, M., Li, J.Y., and Brundin, P. (2010). A simple method for large-scale generation of dopamine neurons from human embryonic stem cells. J. Neurosci. Res. *88*, 3467–3478.

Morizane, A., Doi, D., Kikuchi, T., Okita, K., Hotta, A., Kawasaki, T., Hayashi, T., Onoe, H., Shiina, T., Yamanaka, S., et al. (2013). Direct comparison of autologous and allogeneic transplantation of iPSC-derived neural cells in the brain of a non-human primate. Stem Cell Rep. *1*, 283–292.

Olanow, C.W., Goetz, C.G., Kordower, J.H., Stoessl, A.J., Sossi, V., Brin, M.F., Shannon, K.M., Nauert, G.M., Perl, D.P., Godbold, J., et al. (2003). A double-blind controlled trial of bilateral fetal nigral transplantation in Parkinson's disease. Ann. Neurol. *54*, 403–414.

Ovadia, A., Zhang, Z., and Gash, D.M. (1995). Increased susceptibility to MPTP toxicity in middle-aged rhesus monkeys. Neurobiol. Aging *16*, 931–937.

Pankratz, M.T., Li, X.J., LaVaute, T.M., Lyons, E.A., Chen, X., and Zhang, S.C. (2007). Directed neural differentiation of human embryonic stem cells via an obligated primitive anterior stage. Stem Cells *25*, 1511–1520.

Ramos-Moreno, T., Castillo, C.G., and Martinez-Serrano, A. (2012). Long term behavioral effects of functional dopaminergic neurons generated from human neural stem cells in the rat 6-OH-DA Parkinson's disease model. Effects of the forced expression of BCL-X(L). Behav. Brain Res. *232*, 225–232.

Roggendorf, W., Strupp, S., and Paulus, W. (1996). Distribution and characterization of microglia/macrophages in human brain tumors. Acta Neuropathol. *92*, 288–293.

Sanchez-Pernaute, R., Studer, L., Ferrari, D., Perrier, A., Lee, H., Vinuela, A., and Isacson, O. (2005). Long-term survival of dopamine neurons derived from parthenogenetic primate embryonic stem cells (Cyno-1) after transplantation. Stem Cells *23*, 914–922.

Studer, L., Psylla, M., Buhler, B., Evtouchenko, L., Vouga, C.M., Leenders, K.L., Seiler, R.W., and Spenger, C. (1996). Noninvasive dopamine determination by reversed phase HPLC in the medium of free-floating roller tube cultures of rat fetal ventral mesencephalon: a tool to assess dopaminergic tissue prior to grafting. Brain Res. Bull. *41*, 143–150.

Turovets, N., Semechkin, A., Kuzmichev, L., Janus, J., Agapova, L., and Revazova, E. (2011). Derivation of human parthenogenetic stem cell lines. Methods Mol. Biol. *767*, 37–54.

Vogel, D.Y., Vereyken, E.J., Glim, J.E., Heijnen, P.D., Moeton, M., van der Valk, P., Amor, S., Teunissen, C.E., van Horssen, J., and Dijkstra, C.D. (2013). Macrophages in inflammatory multiple sclerosis lesions have an intermediate activation status. J. Neuroinflammation *10*, 35.

Wilkerson, A., Wongsatittham, K., and Johnston, J. (2013). The NIH stem cell registry: an absence of gamete donor consent. Cell Stem Cell *12*, 147–148.

Xi, J.J., Liu, Y., Liu, H.S., Chen, H., Emborg, M.E., and Zhang, S.C. (2012). Specification of midbrain dopamine neurons from primate pluripotent stem cells. Stem Cells *30*, 1655–1663.

Yoo, J., Kim, H.S., and Hwang, D.Y. (2013). Stem cells as promising therapeutic options for neurological disorders. J. Cell Biochem. *114*, 743–753.